Generation of coherent extreme-ultraviolet and infrared radiation using six-wave mixing in argon

G. Gibson,* T. S. Luk, A. McPherson, and C. K. Rhodes
Laboratory for Atomic, Molecular, and Radiation Physics, Department of Physics, University of Illinois at Chicago, P.O. Box 4348, Chicago, Illinois 60680
(Received 9 April 1990; revised manuscript received 10 September 1990)

Several six-wave mixing processes generating extreme-ultraviolet infrared radiation have been observed in argon gas excited by high-power subpicosecond 248-nm radiation. The processes involve waves over a very large spectral range, spanning the region between 63 nm and 4.3 μm. In addition, two nonparametric transitions are observed whose origin has not been determined

INTRODUCTION

It is well known that lasers can produce many forms of parametric excitation in various materials. One of the simplest and oldest examples of parametric excitation is harmonic generation. With the development of high-power lasers more complex processes have been observed. Indeed, the diversity and subtlety of parametric processes, particularly those driven by high-power lasers, can be bewildering. This paper explores processes of six-wave mixing in argon through which extreme-ultraviolet (EUV) radiation was produced.

Harmonic generation can be thought of as a wave-mixing process involving only the fundamental laser frequency and its harmonics. General wave mixing, on the other hand, can involve waves at any frequency, generating a much richer spectrum of radiation.[1-8] It will be seen from the discussion below that the parametric waves can span a wide spectral range from the infrared (IR) to the extreme ultraviolet (EUV), a region nearly spanning a 100-fold variation in frequency.

Identification of a wave-mixing process is based on two observations. First, the behavior of a parametric wave, i.e., linewidth and intensity as a function of density, should be markedly different from fluorescence lines. Second, the lines suspected of being of parametric origin must fit together to form a consistent parametric scheme. In other words, the parametric loop must conserve energy and this can only be proven through detailed spectroscopic measurements.

In this paper we present evidence for several six-wave mixing processes in neutral argon driven by a high-power ($\sim$0.1–0.25 TW) subpicosecond ultraviolet laser system. Six-wave mixing has been previously observed,[8] but all the wave were sum and difference frequencies of the driving laser and its subharmonics. The experiments discussed here involve the driving laser and a self-generated IR wave. Detailed analysis of four-wave mixing has been attempted by several authors, but inspection shows that the models can become extremely complicated.[1,9,10] Thus, at the level of analysis intended here, we have not attempted to describe the full dynamics of the six-wave processes.

EXPERIMENTAL APPARATUS

The ultraviolet laser system used in these experiments has been described elsewhere.[11] The main component is a custom built KrF* excimer laser which amplifies $\sim$600-fs 248-nm laser pulses up to a single pulse energy of $\sim$150 mJ. The laser was focused with a $f/10$ lens into a vacuum target chamber. The target consisted of a 750-μm bore glass capillary four centimeters long. Argon gas was introduced into the capillary at its midpoint with a pulsed valve. Approximately a millisecond after the capillary was filled with gas, the laser was fired down the bore of the capillary with the focus of the lens located about 2 mm into the structure. The experiment was performed at two densities, estimated to be 2×10^{18} and 6×10^{18} cm^{-3}. In addition, a detailed pressure dependence of one line (63 nm) was obtained.

The average intensity of the laser pulse in the capillary is the power divided by the cross-sectional area of the capillary bore. For the conditions above, the average intensity was $\sim6\times10^{13}$ W/cm^2. The threshold ionization intensity for argon[12] is 3.4×10^{13} W/cm^2. Thus, the processes reported in this work are estimated to have occurred mainly in the intensity range spanning 10^{13}–6×10^{13} W/cm^2, a region presumably accompanied by an appreciable level of ionization of the medium.

The EUV radiation emitted along the axis of the capillary was recorded[13] with a resolution of $\sim$1.4 Å and an absolute wavelength calibration of $\pm$0.3 Å. Based on previous experience[1] and initial conjectures based on the observed EUV spectrum, the IR spectrum was thought to be important. Consequently, it was recorded with a 0.3-m McPherson normal incidence monochromator with either a 75 or a 300 lines/mm grating. The entrance slit of the IR monochromator was 750 μm. The resolution was approximately 0.04 μm with the 75 lines/mm grating and 0.01 μm with the 300 lines/mm grating. The spectral ranges recorded were from 4.0 to 5.7 μm and from 2.0 to 4.0 μm with the 75 and 300 lines mm gratings, respectively. The absolute wavelength calibration was $\pm$0.005 μm.

RESULTS AND DISCUSSION

The spectrum recorded from the capillary consisted of only a few strong features both in the IR and EUV spec-

tral regions, as shown in Fig. 1. Various properties of all the lines observed in argon are listed in Table I, including the properties of the laser radiation (ω_L) itself. Four important characteristics of the radiation in Table I are apparent: (1) compared to spectra of fluorescence,[13] relatively few lines are seen; (2) most of the lines are quite broad; (3) close inspection showed that several of the wavelengths were not exactly constant from one run to the next; and (4) many of the wavelengths do not match known atomic transitions. All of these characteristics are suggestive of a parametric origin for the majority of the radiation seen. The errors in the energies in Table I were influenced by points (2) and (3) above. For the sharp lines, the errors represent the absolute accuracy of the spectrometer. The larger errors on certain features reflect the width and fluctuations of the feature. The feature labeled *a* in Fig. 1(a) was influenced by a well-known[14] absorption band of CO_2. The width and magnitude of the absorption band is consistent with typical concentrations of CO_2 in the atmosphere. However, feature *a* is much broader than the absorption band.

An understanding of the spectrum observed depends on the energy level structure[15] of argon shown in Fig. 2(a). The most important feature to note is the almost perfect three-photon resonance of the laser with the 4*d* level manifold. All of the 4*d* states are accessible from the ground level, since the three photons making the transition can provide up to three units of angular momentum. This resonance can generate third-harmonic ($3\omega_L$) radiation, but, more importantly, it can also drive various other wave-mixing processes.

The next important observation from Table I concerns the simultaneous presence of both the 63- and 128-nm components, neither of which match a known transition in argon. However, the difference in energy between these two waves, $80\,605\pm300$ cm^{-1}, is twice the energy of one laser photon ($\omega_L = 40\,258\pm35$ cm^{-1}). Thus, these two waves appear to be anti-Stokes and Stokes scattering, respectively, of the laser off of some intermediate excited

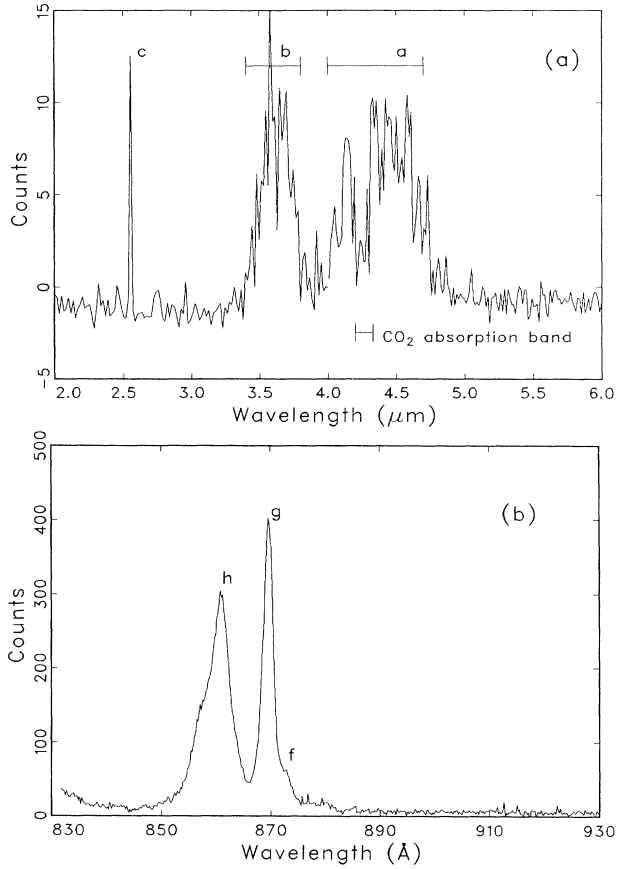

FIG. 1. (a) IR spectrum from capillary. There is a break in the spectrum at 4 μm corresponding to a change of gratings. The grating efficiency falls off from 4.5 to 4 μm and, thus, the central wavelength of the feature around 4.5 μm is actually estimated to be at 4.3 μm. The dip in the spectrum at $\sim$4.26 μm is due to atmospheric absorption of CO_2. (b) EUV spectrum from the capillary. In addition, radiation was also observed at 63, 128, and 82.8 nm, the latter being the third harmonic. The feature at 87.1 nm is relatively weak in this spectrum.

TABLE I. Observed radiation in argon.

	Wavelength[a]	Energy (cm^{-1})	Width (cm^{-1})	Comments	Source of dispersion for radiation in the six-wave processes
a	4.3 μm	$2\,353\pm100$	300	ω_{IR}: $3\omega_L - 5p^*$	High density of free electrons
b	3.60 μm	$2\,778\pm40$	300	No explanation	
c	2.57 μm	$3\,906\pm8$	≤ 17	Not parametric: $5p[1/2]_0 \rightarrow 5s[1/2]_1^0$	
d	248.4 nm	$40\,258\pm35$	40	KrF* laser: ω_L	Nonlinear, self-induced
e	128 nm	$78\,125\pm60$	120	Six-wave process: $5p^* - \omega_L$	Weak, nonresonant
f	87.1 nm	$114\,810\pm150$	400	No explanation, but weak	
g	86.96 nm	$114\,995\pm60$	≤ 100	Not parametric: possibly satellite line or $5s[1/2]_1^0 \rightarrow 3p^6$	
h	86 nm	$116\,279\pm150$	300	Six-wave process: $5p^* - \omega_{IR}$	Resonance from 5*s* and 3*d* neutral argon levels
i	82.8 nm	$120\,774\pm100$	100	Third harmonic: $3\omega_L$	Resonance from the 3*d* neutral argon levels
j	63 nm	$158\,730\pm250$	500	Six-wave process: $5p^* + \omega_L$	Continuum above the neutral ionization potential

[a]This alphabetic label is used to mark the spectra in Fig. 1.

state to a common lower level, presumably the atomic ground state. Averaging the energy of the two waves determines the energy of the intermediate state, placing it at 118 427±150 cm^{-1}. Although this could be a virtual state, a real bound level in the atom would be expected to be close. In fact, three $5p$ energy levels are grouped near this value, and, hence, this experimentally determined level will be referred to as the $5p^*$ level. The intensity at which these processes are occurring could be sufficient to create a significant a.c. Stark shift in the zero-field levels.[16] Thus, the energy of the level deduced from the observed waves need not agree exactly with the known, zero-field states.

The next question concerns the mechanism populating the $5p^*$ level. The $5p^*$ state lies just below the energy of the third harmonic ($3\omega_L$), and, perhaps, could be connected to this wave, if an additional photon were participating to satisfy the constraint of parity. The difference between $3\omega_L$ and the $5p^*$ level is 2347±200 cm^{-1}. It would be expected that initially the three-photon resonant $4d$ level will be inverted with respect to the $5p^*$ level. Thus, a stimulated wave could develop at the difference frequency corresponding to a wave at 4.3±0.2 μm. In fact, energy at this wavelength is present in Fig. 1 and an entry corresponding to this wave is included in Table I (ω_{IR}). It is this wave which populates the $5p^*$ level and leads to the Stokes and anti-Stokes scattering at 248 nm discussed above. In summary, the complete six-wave process proceeds as follows. A self-generated infrared wave (ω_{IR}) is produced by electronic hyper-Raman scattering of three laer photons ($3\omega_L$) off of the near-resonant $4d$ levels. This leaves the atom in the excited $5p^*$ state. Anti-Stokes and Stokes scattering of the laser off of the $5p^*$ state returns the atom to its ground state, generating waves at 63 and 128 nm, respectively. These six-wave loops are shown in Fig. 2(a).

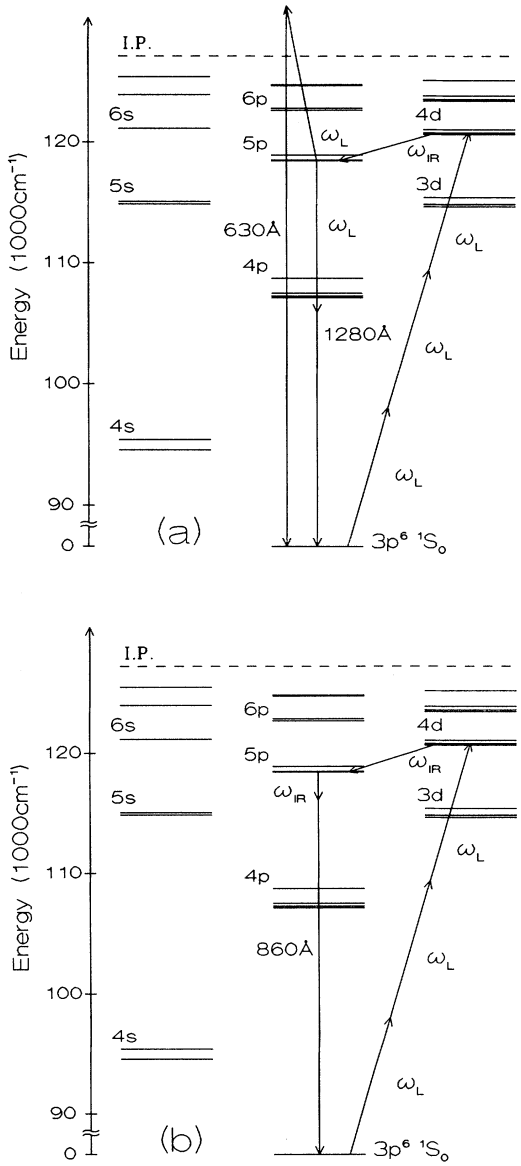

FIG. 2. Argon energy level diagram showing the six-wave mixing schemes. (a) Stokes and anti-Stokes scattering of the laser off of the $5p^*$ level. (b) Scattering of the IR wave off of the $5p^*$ level. IP denotes ionization potential.

Besides the two loops discussed above, there is yet another possibility. Since the IR wave (ω_{IR}) is real radiation, it too can scatter off of the $5p^*$ level.[1] Anti-Stokes scattering would result in a frequency of $3\omega_L$ and would be indistinguishable from the third harmonic. Stokes scattering, however, would generate a new wave at 116 080±300 cm^{-1} (86 nm). This closely matches an observed line (86 nm) in Table I and thus closes a third six-wave loop: $3\omega_L$ up, $2\omega_{IR}$ down, and 86 nm down, as shown in Fig. 2(b).

Although the dynamics of the six-wave–mixing process was not systematically investigated, some interesting properties of the 63-nm line, as a function of gas density, are shown in Figs. 3 and 4 to contrast its behavior with a known fluorescence line from neutral argon ($3p^6$-$3p^5(^2P_{3/2}{}^\circ)4s$, 106.7 nm). In particular, the parametric 63-nm line shows a very rapid increase with density as opposed to the initially linear increase of the fluorescence line. Furthermore, the linewidth of the 63-nm line changed greatly with density whereas the width of the fluorescence line was always that of the spectrometer resolution.

At phase matching affects all aspects of the dynamics of parametric process, it must first be understood before any quantitative analysis is possible. Even in a simpler case of harmonic generation at high intensities the question of phase matching prevented a clear understanding of the data.[17] Table I details the contributions to the dispersion of the waves in the six-wave processes. In addition, it has been observed that the intensity of the 248-nm wave is sufficient to introduce a nonlinear dispersion, not only at 248 nm, but at all frequencies.[18] Clearly, it is extremely difficult to determine the overall phase matching conditions in this complex situation.

In addition to the rather broad features listed in Table I, there are two lines which are as narrow as the instrumental resolution and, thus, appear to have an origin different from the mechanism described above. The sharpness of these lines would suggest that they result

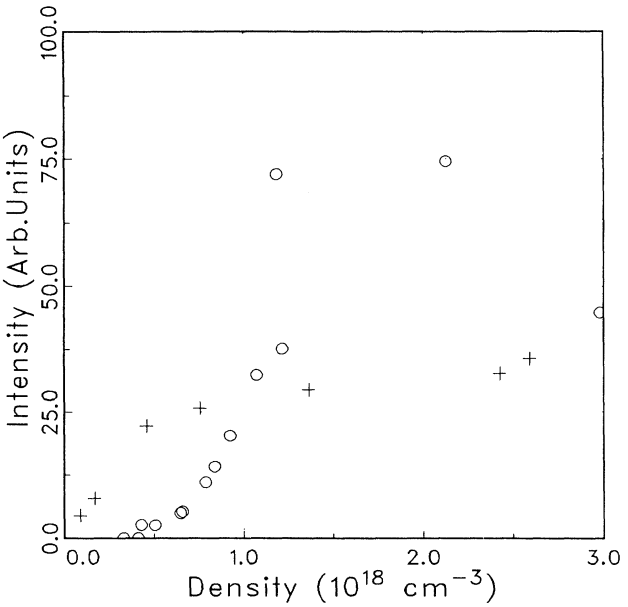

FIG. 3. Pressure dependence of the integrated intensity of 63-nm line (○), and a neutral argon (106.7 nm) fluorescence line (+).

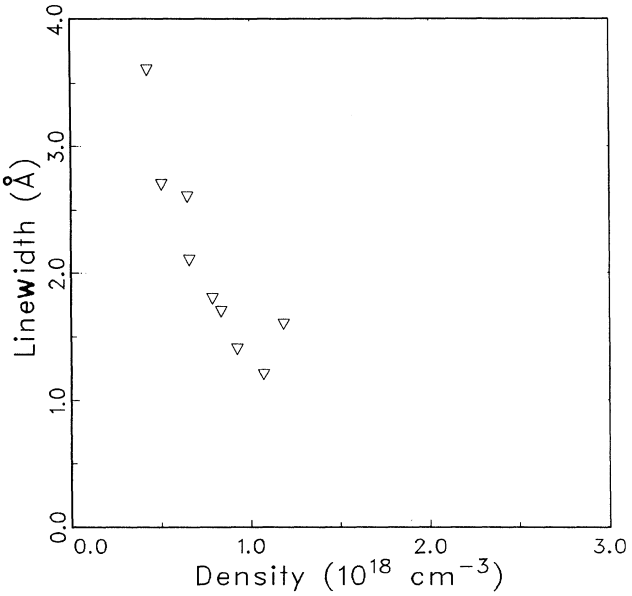

FIG. 4. Pressure dependence of the linewidth of the 63-nm line (▽).

from transitions between real atomic states. In fact, the IR line at 2.57 μm matches the known $5p[1/2]_0 \rightarrow 5s[1/2]_1^0$ laser transition[19] to within the wavelength calibration of the spectrometer. Efficient population of the upper state, $5p[1/2]_0$, could result from the transfer of population from the three-photon resonant $4d$ levels. This transfer could take place through collisions or radiative decay of the $4d$ levels. For the latter, the radiation would have a wavelength of 5.78 μm, a value beyond the range of our detector. Thus, it was not possible to determine the mechanism leading to the apparent population of the $5p[1/2]_0$ state.

The other conspicuous narrow line in Table I, occurring at 86.96 nm, matches the $5s[1/2]_1^0 \rightarrow 3p^6$ transition in neutral argon,[20] again to within the wavelength calibration of the spectrometer. The upper state for this line is exactly the lower state of the 2.57-μm transition, a situation suggesting that these two transitions could be connected as a cascade. However, several considerations are expected to reduce significantly the radiative efficiency of the $5s[1/2]_1^0 \rightarrow 3p^6$ transition under the conditions studied. They are radiation trapping of the 86.96-nm line and destruction of the upper level by collisional processes, including argon excimer formation governed by a relatively large three-body rate constant[21] of 2.5×10^{-31} cm^6/s.

Based on the known spectroscopy of argon,[20] there is a second possible origin of the 86.96-nm feature. It involves an unclassified transition observed at 86.92 nm, a wavelength that agrees,within the instrumental resolution, with the entry in Table I. Since such a transition could arise as a satellite line, which is unlikely to involve ground-state species of either the neutral atom or atomic ions, it would not experience trapping and could radiate freely. However, without further information on the identification of the level involved, no statement on the nature of the mechanism potentially leading to its population can be made at this writing.

On the basis of the experimental data, it has not been possible to associate either the 2.57-μm or 86.96-nm spectral components with parametric mechanisms. Furthermore, two additional features included in Table I, occurring at 3.60 μm and 87.1 nm, cannot be accounted for by the schemes presented above. Possibly, they indicate some other aspect of the nonlinear coupling on the presence of related additional high-order nonlinear processes, perhaps of a greater order than the six-wave mechanism presented.

In conclusion, argon irradiated with intense subpicosecond 248-nm radiation in a capillary structure can give rise to EUV radiation from six-wave parametric processes involving the participation of waves over a very extended spectral range. In addition to the parametrically generated waves, certain observed spectral components in both the EUV and IR ranges appear to arise from other mechanisms whose origin will require further study.

ACKNOWLEDGMENTS

The technical assistance of P. Noel and J. Wright and fruitful discussions with K. Boyer are acknowledged. Support for this research was provided by the U.S. Air Force Office of Scientific Research, the U.S. Office of Naval Research, and the Strategic Defense Initiative Organization.

*Present address: AT&T Bell Laboratories, Murray Hill, NJ 07974.

[1]M. Shahidi, T. S. Luk, and C. K. Rhodes, J. Opt. Soc. Am. B **5**, 2386 (1988).

[2]K. D. Bonin and T. J. McIlrath, J. Opt. Soc. Am. B **2**, 527 (1985).

[3]R. Hilbig and R. Wallenstein, IEEE J. Quantum Electron. **QE-19**, 194 (1983).

[4]F. S. Tomkins and R. Mahon, Opt. Lett. **6**, 179 (1981).

[5]J. Bokor, R. R. Freeman, R. L. Panock, and J. C. White, Opt. Lett. **6**, 182 (1981).

[6]R. R. Freeman, J. Bokor, and W. E. Cooke, Phys. Rev. A **26**, 3029 (1982).

[7]K. W. Lugewigt, W. Pfingsten, C. Mohlmann, and B. Wallegehausen, Opt. Lett. **11**, 39 (1987).

[8]J. Rentjes, C. She, and R. C. Eckardlt, IEEE J. Quantum Electron. **QE-14**, 581 (1978).

[9]R. Boyd, M. Malcuit, and D. Gauthier, Phys. Rev. A **35**, 1648 (1987).

[10]J. F. Reintjes, *Nonlinear Optical Parametric Processes in Liquids and Gases* (Academic, New York, 1984).

[11]T. S. Luk, A. McPherson, G. Gibson, K. Boyer, and C. K. Rhodes, Opt. Lett. **14**, 1113 (1989).

[12]G. Gibson, T. S. Luk, and C. K. Rhodes, Phys. Rev. A **41**, 5049 (1990).

[13]A. McPherson, G. Gibson, H. Jara, U. Johann, T. S. Luk, I. A. McIntyre, K. Boyer, and C. K. Rhodes, J. Opt. Soc. Am. B **4**, 595 (1987).

[14]G. Herzberg, *Molecular Spectra and Molecular Structure II. Infrared and Raman Spectra of Polyatomic Molecules* (Van Nostrand, Princeton, New Jersey, 1945), p. 273.

[15]C. E. Moore, *Atomic Energy Levels* (U.S. PO, National Bureau of Standards, Washington, D.C., 1971), Vol. 1.

[16]H. Pummer, H. Egger, T. S. Luk, T. Srinivasan, and C. K. Rhodes, Phys. Rev. A **28**, 795 (1983).

[17]L. A. Lompré, A. L'Huillier, M. Ferray, P. Monot, G. Mainfray, and C. Manus, J. Opt. Soc. Am. B **7**, 754 (1990).

[18]R. Rosman, G. Gibson, K. Boyer, H. Jara, T. S. Luk, I. A. McIntyre, A. McPerson, J. C. Solem, and C. K. Rhodes, J. Opt. Soc. Am. B **5**, 1237 (1988).

[19]W. L. Faust, R. A. McFarlane, C. K. N. Patel, and C. G. B. Garrett, Phys. Rev. A **133**, 1476 (1964).

[20]R. L. Kelly, J. Phys. Chem. Ref. Data **16**, Suppl. No. 1 (1987).

[21]K. T. Gillen, R. P. Saxon, D. C. Lorents, G. E. Ice, and R. E. Olson, J. Chem. Phys. **64**, 1925 (1976).